scientific reports

OPEN

Research on the mechanism and technology of close range coal seam support and roof cutting collaborative lane control

Wanpeng Huang[1], Yaxin Liu[1], Tongyang Zhao[1✉], Le Sui[2], Xinyu Chu[1] & Lingzhuo Zhu[1]

Due to rock damage in close-range tunnels and difficulty controlling stability, proposes a precise surrounding rock control concept of goaf-retaining roadways in close-range without coal pillars. A mechanical model for the load transfer of overlying rock strata in the goaf under the roof cutting structure of the roadway is constructed, and a precise quantitative support design method for the surrounding rock without coal pillars is formed, with the main steps being the mechanical rock properties research, the design of support strength, and the optimization of support structure schemes. To clarify the mechanical properties of high-strength support structures for steel-reinforced concrete pillars, indoor tests were conducted on long pillar supports with different aspect ratios to analyse the deformation failure modes and bearing performance of long pillars. Through numerical simulation, the peak support pressure of the roadway was reduced by 41.2% due to coordinated support and cutting, effectively reinforcing the roof and cutting off the stress transmission path. The deformation and failure control laws of the surrounding rock with different support schemes for goaf-retaining roadways in close-range were revealed. Successful application at Xinchazhuang coal mine significantly improved the stability control of the surrounding rock in the goaf compared to traditional support techniques.

In regions such as North China, Northwest China, Northeast China, and Southwest China, coal resources are abundant, and there are generally multiple layers of coal seams in the coal-bearing strata. Among them, there are numerous mineable coal seams with small vertical spacings, mostly belonging to close or extremely close range coal seam groups[1,2]. However, in the process of close range coal seam mining, there are two long-standing difficulties. First, the protective coal pillars left in each coal seam mining section often have a significant impact on adjacent coal seam mining, causing significant local stress concentration in the affected area of the coal pillars, leading to increased support difficulty and weakened support effectiveness[3–5]. The second problem is that the retention of coal pillars leads to a decrease in extraction rates, resulting in a significant waste of resources and increased costs[6,7].

Therefore, due to the increasing scarcity of coal resources, studying the safe and efficient mining of close range coal seams without coal pillars has considerable practical significance[8]. Although free coal pillar technology has achieved successful experimental results in coal seams under various conditions, the stress environment during close range mining of low coal seam goafs is complex, the mining pressure is severe, the roadway roof bends and sinks, the support seriously bulges, and the metal mesh is damaged, which induces large deformation of the surrounding rock and increases the difficulty of controlling the surrounding rock of the goaf, as shown in Fig. 1[9,10]. Many scholars worldwide have conducted effective research on migration laws and support control of overlying strata in close range coal seam mining to solve the problems of close range coal seam mining and promote the development and application of close range coal seam mining technology[11–14]. In terms of the evolution of the surrounding rock stress, Yang et al.[15] studied the stress and deformation evolution law of the overlying rock strata in the roof cutting of a close range coal seam retaining roadway, the roof stress of the upper coal seam experienced cyclic unloading–reloading stress and that the stress of the high-level roof increased,

[1]College of Energy and Mining Engineering, Shandong University of Science and Technology, Qingdao 266590, Shandong, China. [2]School of Mechanical and Electrical Engineering, China University of Petroleum (East China), Qingdao 266580, China. ✉email: tongyangz@163.com
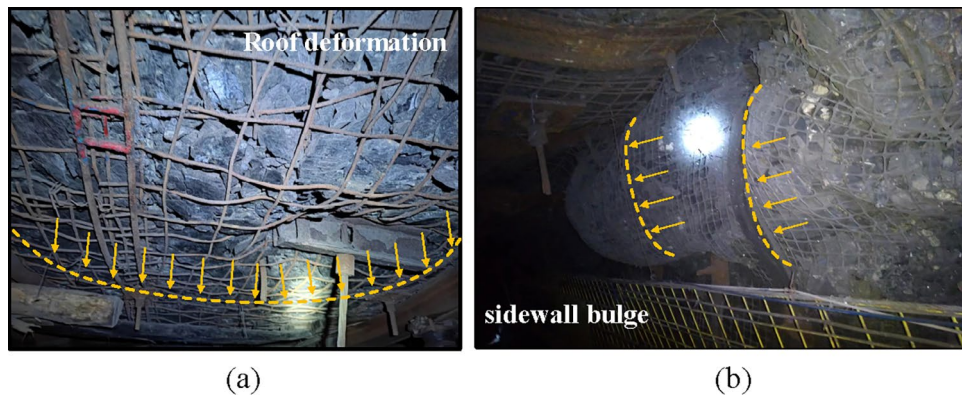
Fig. 1. Deformation of surrounding rock (Xinchazhuang Coal Mine).

resulting in increased stress. In terms of stress transfer in surrounding rock, Zhao[16] verified that the use of hydraulic fracturing can reduce the stress disturbance effect of overlying coal pillars on the lower coal seam during close range mining. Ma et al.[17,18] demonstrated that directional presplitting blasting achieves roof fracture control and structural integrity preservation in pillarless mining operations. In terms of surrounding rock control, Ma et al.[17,18] reported that the "anchor cable + single pillar + filling wall" support scheme can effectively control the subsidence of the roadway roof and proposed the "improving the support strength to achieve roof cutting" support concept. Zhang et al.[19] proposed key technologies such as the "trinity" of precracking and pressure relief, zoning treatment, and optimization of structural parameters for controlling the surrounding rock of goaf-retaining roadways.

The above research shows that reasonable stress transfer of the overlying rock structure and high-strength support technology are the keys to maintaining the stability of the surrounding rock of this type of roadway[20]. This article focuses on the scientific and technological challenges of high roof rock pressure and large deformation of the surrounding rock in close range coal seam goaf retention. Taking the close range coal seam in the Xinchazhuang Coal Mine as the research object, a collaborative control technology system for roof cutting and pressure relief and high-strength support beside the roadway is proposed. The structural migration characteristics of the surrounding rock in the roof cutting of close range goaf retention roadways and pressure relief are studied. Combined with the high-strength mechanical properties of steel-reinforced concrete pillars, an optimization scheme for high-strength control of the surrounding rock in a close range goaf-retention roadway is determined and is successfully applied in the 91006 track trench for practical engineering, providing a reference for the promotion and application of similar geological conditions in mines.

Project overview

Shandong Xinchazhuang Mining Co., Ltd., is located in Shiheng town, Feicheng city, Shandong Province, China, and is under the jurisdiction of Feicheng city. The 91,000 deep mining area is adjacent to the overlying 8800 mining area from the west to the F27 fault. Adjacent to the CF87 fault and 91,000 mining area in the south, the CF3 fault in the north is adjacent to the overlying 81,100 mining area, and coal 8 overlying coal 9 in the mining area is recovered. Approximately 7.5 m below the 8th coal seam is the 9th coal seam, which is a close range coal seam. The plan for the stacking relationship between the 8th and 9th coal seams is shown in Fig. 2. The development of tunnels in the Xinchazhuang Coal Mine involves a large amount of work and tight production continuity, which severely affects the production continuity of the mining area and even the entire mine. Therefore, work on the retaining roadway along the goaf will be carried out on the 91006 working face of the 9th coal seam, and the proposed retained roadway will be the track groove of the 91006 working face.

The track groove of the 91006 working face is located at a level of − 350 m in the lower coal mining area, the upper and lower limits of the roadway have elevations ranging from − 459.89 to − 482.5 m. The design length of the 91006 track groove is 448 m, and the coal (rock) layer within the construction range has a roughly northwest direction and a northeast inclination, with an average dip angle of approximately 6°. The rock layers between coal seam 9 and coal seam 8 are composed of mudstone, sandstone, siltstone, and marl. Core drilling and indoor rock mechanics tests were conducted on site, and the structure and mechanical parameters of the roof and floor are shown in Table 1.

In the design of the track groove of the 91006 working face, the roadway is excavated along the roof of coal 9. When the thickness of the mudstone on the roof is greater than or equal to 0.7 m or less than 0.7 m, different support schemes are used. The cross-sectional structure and support schematic diagram of the overlying rock after leaving the roadway are shown in Fig. 3. The design parameters for the roadway section support are shown in Table 2.

Control concept and method of retaining the roadway along the goaf of a close range coal seam

To alleviate the influence of disturbing factors such as stress transfer between the lower layers and collapse of the goaf during mining of the upper coal seam, research has been carried out from two aspects: advanced roof
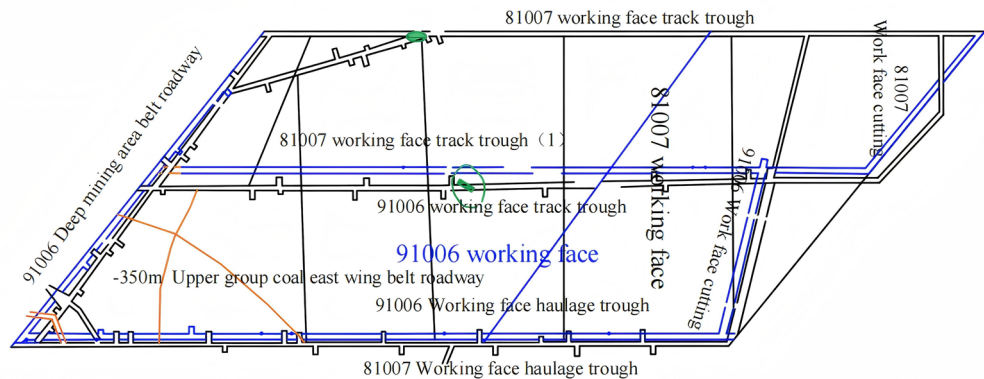
Fig. 2. 8, 9 coal face superposition relationship plan.

cutting and pressure relief technology, which changes the structure of the upper rock strata and high-strength support beside the roadway. The joint control technology of roadway roof cutting and high-strength restraint under close range conditions is proposed. The control concept includes advanced roof-breaking pressure relief, high-strength support constrained by the surrounding rock surface, and isolation of the goaf, as shown in Fig. 4. The roof cantilever force transmission structure is actively changed by roof cutting, and the high-strength support of the concrete-filled steel tubular pillars is combined to strengthen the roof support of the roadway to jointly control the stability of the surrounding rock.

Principles of advanced roof cutting and pressure relief technology

After close range coal seam mining, the overlying rock structure breaks and moves, resulting in a new stable structural state of the overlying rock. The mining stress generated by the working face of the upper coal seam during the mining process is transmitted downstream in the rock layers between the upper and lower coal seams, and the load of the goaf gangue and overlying rock is also borne by the rock layers between the upper and lower coal seams. The propagation path of mining-induced stress passes through the high-stress mining source in the upper coal mining area, and the rock layer path is subsequently transmitted through the space between the close range coal seams to the bearing structure. During the mining of the lower coal seam, according to classical mining pressure theory, without prior treatment of the immediate roof above the coal seam, the immediate roof fractures periodically with mining of the working face. The fracture position is located above the solid coal side, forming a long cantilever beam structure[21], as shown in Fig. 5a. Under the roof fracture structure, the immediate roof of the fracture is jointly borne by the solid coal support, support structure, and fallen gangue in the goaf. To effectively control the stability of the surrounding rock in a roadway, in-depth research can be conducted on removing mining-induced stress sources, changing the load transmission path for stress isolation, or improving support strength.

The advanced roof-breaking and pressure relief technology for close range goafs can change the movement of overlying rock layers and weaken the force of the roadway roof by cutting the roof in the goaf and destroying its overall structure, thereby further changing the load path of mining stress under the goaf. On the other hand, the overlying rock layer breaks and collapses along the presplitting line, and the broken rock blocks accumulate in the goaf. The arc-like triangular hanging plate structure on the goaf side of the coal pillar is artificially destroyed, causing the roof-breaking structure above the coal seam to change from the original one-end fixed support and one-end hinged rock beam to a short cantilever beam structure with one-end fixed support and one end free, reducing the length of the hanging roof and reducing the additional load applied to the support of the roadway, playing a role in relieving pressure and protecting the roadway along the goaf, as shown in Fig. 5b.

Principle of high strength support technology for road sides

Advanced roof-breaking and pressure relief technology can effectively change the lateral structure of the roof and reduce the original abutment pressure beside the roadway. However, for the goaf in the upper coal seam of the near seam, the roadway side support needs to bear not only the upper rock beam structure but also all the caving dead weight of the upper coal seam, which requires high bearing capacity beside the roadway and high-strength roadway side support to effectively control roof caving. By filling hollow steel pipes with high-strength concrete, the concrete-filled steel tube (CFST) pillars can bear the joint load of an external high-strength constraint structure and internal core concrete force to ensure that the improvement in the compressive strength of the core concrete and the external constraint structure cannot destabilize, with complementary advantages[22]. A flexible cushion structure is located above the pillar, which buffers and allows pressure and realizes the combination of rigid and flexible support structures. The high-strength support of CFST pillar is shown in Fig. 6.
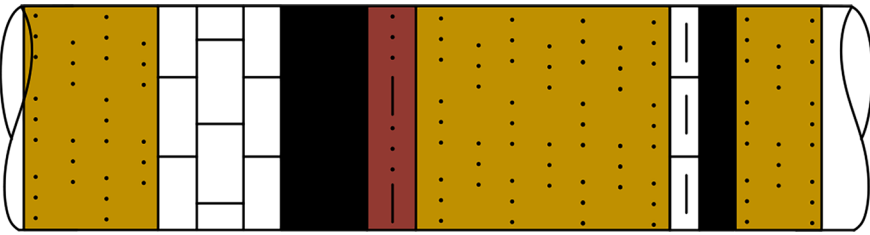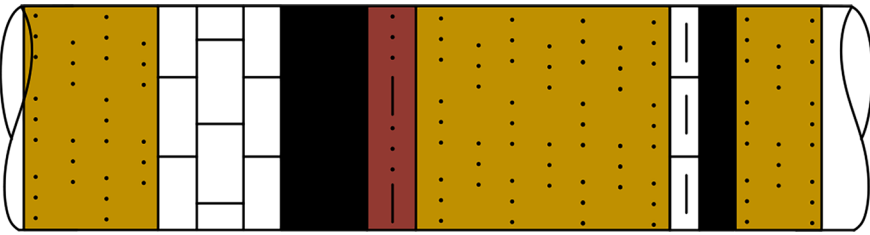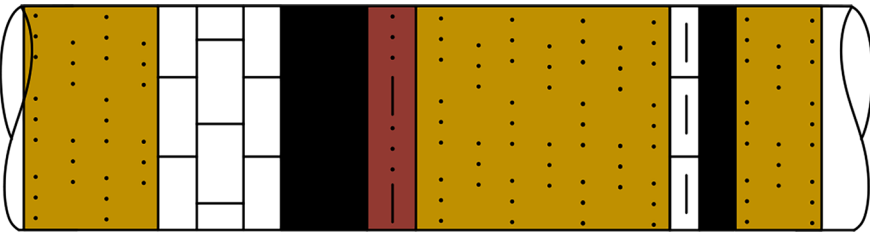
| Lithology		Thickness	Compressive strength/MPa	Tensile strength/MPa	Cohesion/MPa	Elastic modulus/GPa	Poisson ratio	Density/kg/m³
Siltstone		2.1–5.6 / 4.0	117.88	4.57	11.07	18.09	0.36	2526.8
Fourth limestone layer		3.0–5.5 / 4.2	129.51	10.97	7.26	19.11	0.23	2671.1
8 Coal		1.8–2.3 / 2.1	15.19	1.44	0.42	1.84	0.29	1325.5
Pelitic siltstone		0.8–1.2 / 1.0	59.64	3.60	1.7	6.18	0.28	2543.4
Siltstone		4.5–6.5 / 5.8	117.88	4.57	11.07	18.09	0.36	2526.8
Mudstone and limestone		0–1.5 / 0.7	106.96	8.66	16.6	16.94	0.41	2494.4
9 Coal		1.1–1.4 / 1.3	9.55	0.64	4.08	1.45	0.19	1310.2
Siltstone		2.5–3.7 / 3.1	117.88	4.57	11.07	18.09	0.36	2526.8

Table 1. Structure and mechanical parameters of roof and floor.
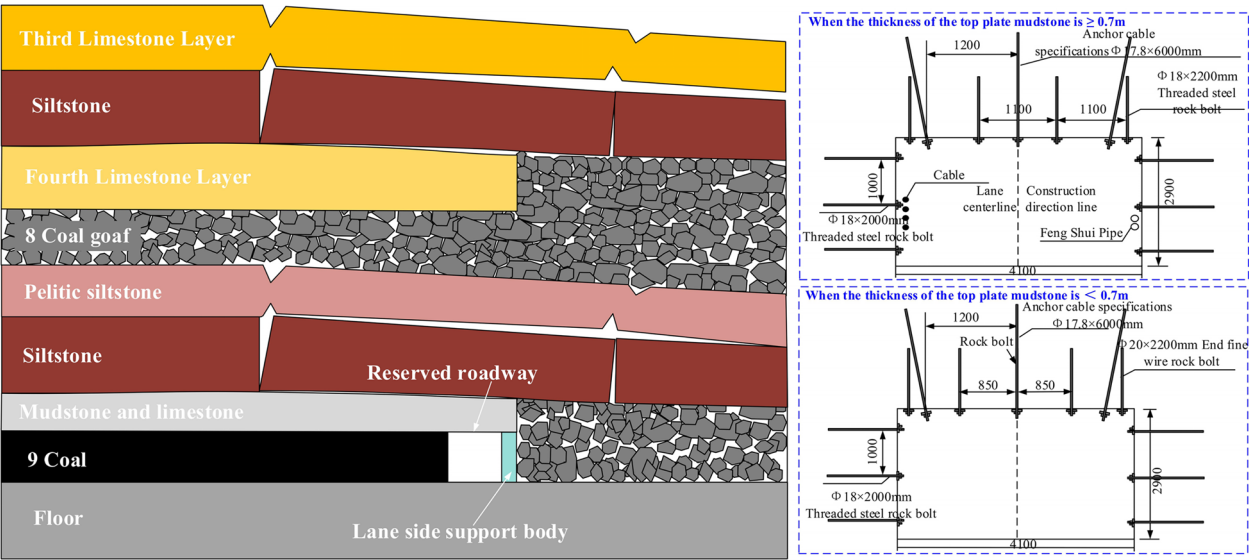
Fig. 3. Schematic diagram of the cross-section structure and support of the overlying rock.

| Design scheme	Design parameters	
Bolt-cable support	The thickness of the top plate mudstone ≥ 0.7 m	The top rock bolt size is Φ18×1600 mm, with the spacing and row is 1100×2600 mm. Anchor cable size is Φ17.8×5000 mm, with the spacing and row is 1200 mm×3000 mm. The side bolt size is Φ18×2000 mm, with with the spacing and row is 800×1000 mm
	The thickness of the top plate mudstone < 0.7 m	The top rock bolt size is Φ20×2200 mm, with the spacing and row is 850×1000 mm . Anchor cable size is Φ17.8×5000 mm, with the spacing and row is 1200 mm×3000 mm. The side bolt size is Φ18×2000 mm, with with the spacing and row is 800×1000 mm

Table 2. Support design parameters.
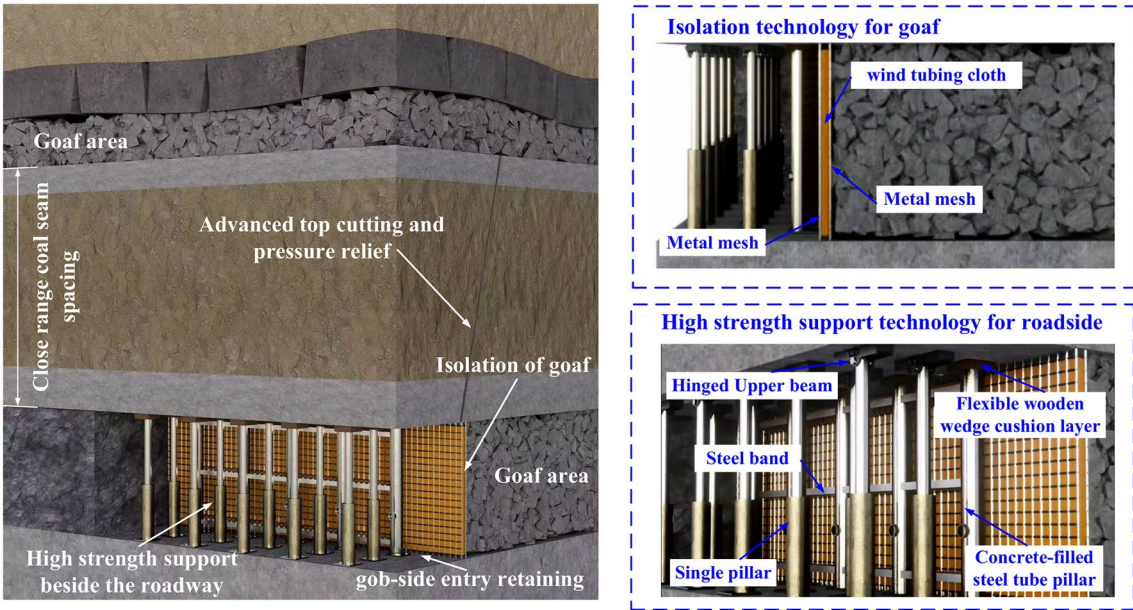
Fig. 4. Top cutting and high-strength constraint control technology for close range goaf roadway (created by Maxon Cinema 4D version 25; https://www.maxon.net/en/cinema-4d).

Research on advanced roof-breaking schemes and parameters for close range coal seams

Hydraulic fracturing and top cutting technology and parameter analysis

To reduce the impact of the mining load on goaf retention in the lower coal seam, hydraulic fracturing
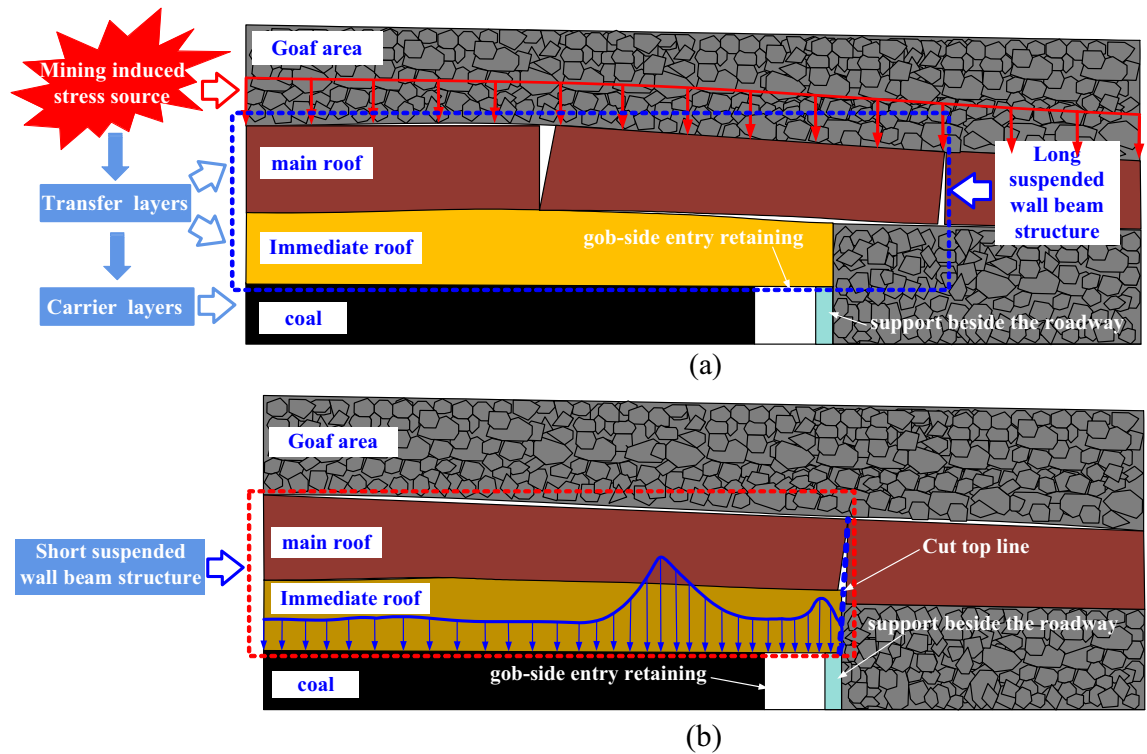
(a)

(b)

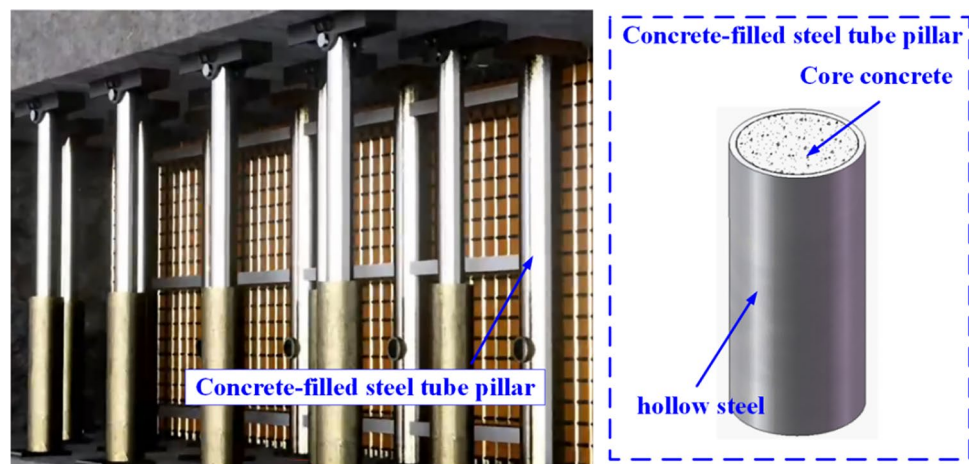**Fig. 5**. Schematic diagram of the surrounding rock structure of the roadway left in gob-side.

Fig. 6. Schematic diagram of high-strength support of CFST pillar (created by Maxon Cinema 4D version 25; https://www.maxon.net/en/cinema-4d).

technology is used to change the stress distribution and stress transfer. By drilling holes a certain distance from the advancing working face near the goaf side of the roadway, the pressure crack holes continue to expand under the action of high water pressure, resulting in the continuous expansion of cracks in the rock layer, changing the macro- and microstructures of the rock mass, and thus weakening the mechanical properties of the rock mass. Moreover, the mechanical properties of rocks are reduced by the physical and chemical action of water on rocks[23]. With the advancement of the working face, the roof weakens by fracture breaks and collapses in time, and the gob is compacted in time. After the main roof rock fractures, the abutment pressure level of the working face decreases, and the stress distribution becomes more uniform. The fracture top pressure relief characteristics of hydraulic fracturing are shown in Fig. 7.

Holes were drilled diagonally towards the working face in the 91006 track roadway, perpendicular to the roadway, and were located in the shoulder groove, facing the roof of the working face. To achieve rock fracturing and weakening, the focus was on fracturing the 5.8 m sandstone layer. The drill holes were fractured every 3 m,
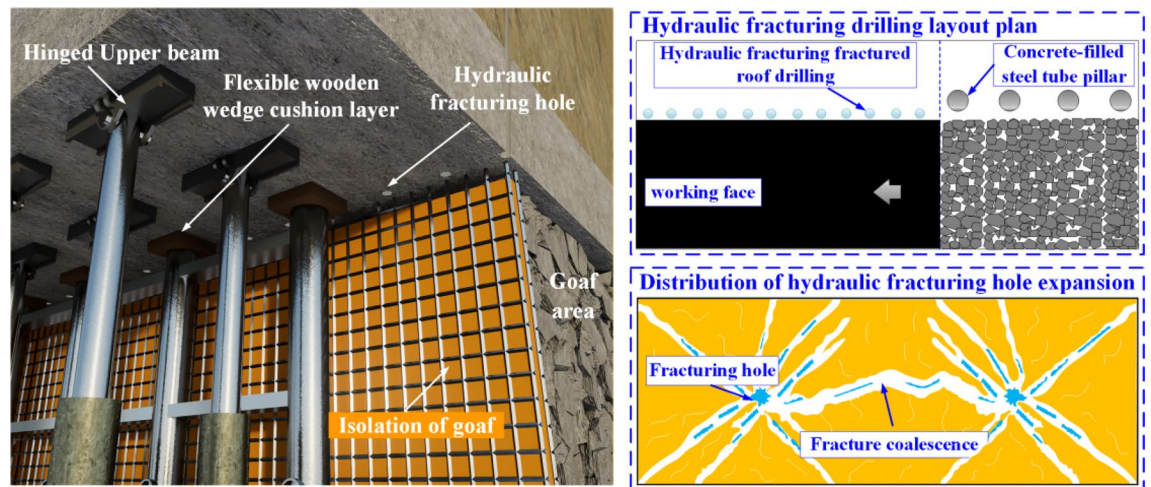
Fig. 7. Schematic diagram of hydraulic fracturing top breaking and pressure relief.

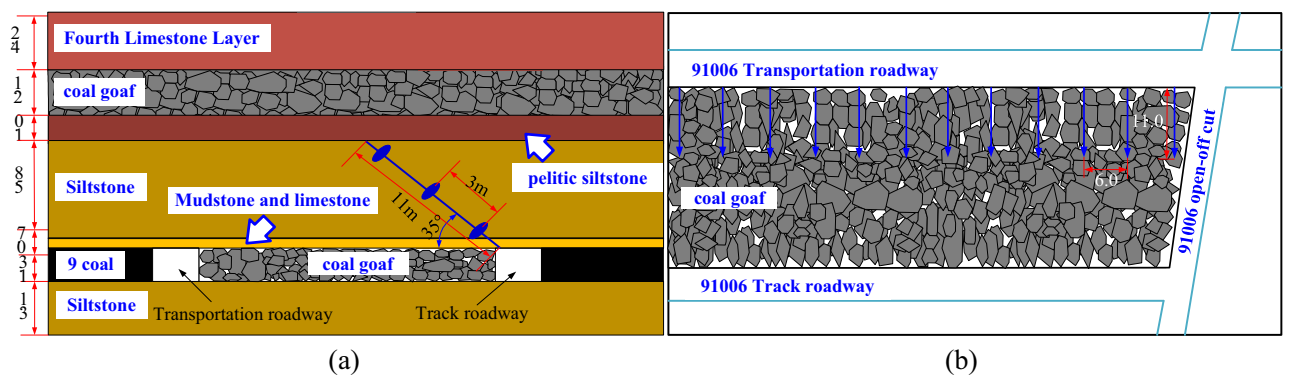(a)   (b)

Fig. 8. Schematic diagram of hydraulic fracturing drilling layout.

with each hole being fractured twice. The fracturing time for each segment is controlled at 30 min, with a water pressure of 30–34 MPa, the drill hole diameter of 65 mm, the drill hole length of 11 m, the angle of 35°, and the drill hole spacing of 6 m. The drill hole layout is shown in Fig. 8.

Calculation of the resistance of roadside support

After mining of the front working face is finished, the rock above the coal pillar side of the goaf experiences immediate roof fracture. A model of the mechanical structure of the overlying rock movement characteristics along goaf retaining roadway is established by using the limited deformation mode under roof unloading, as shown in Fig. 9. In this mode of the overlying rock structure, the self-weight of the short cantilever beam is small, and there is no large pivotal subsidence. The self-weight of the rock beam is jointly borne by the solid coal wall and the side supporting body of the roadway, and the side supporting body is supported by a high-strength concrete-filled steel tube. It can effectively control the rotation and settlement of the main roof so that the main roof cannot settle to the lowest state.

Based on the above analysis, the weights of the hanging parts of the direct roof and immediate roof rock formations above the track roadway of the 91006 working face, as well as the weight of the goaf caused by the collapse of the direct roof and immediate roof of the No. 8 coal seam, are all borne by the roadway support body. According to the moment balance analysis, the formula for the support pressure that the roadway support body needs to bear is[24]:

$$F = \frac{1}{2}\sigma L = \frac{1}{2}L\sum_{i=1}^{n} K_x y_i m_i \tag{1}$$

where F is the supporting pressure beside the roadway; σ is the self-weight load of the overlying rock layer directly at the top and the main roof; L is the length of the overhang covering the top plate above; y_i is the bulk density of the rock layer; m_i is the thickness of each rock layer above the coal seam; and K_x is the stress concentration factor.
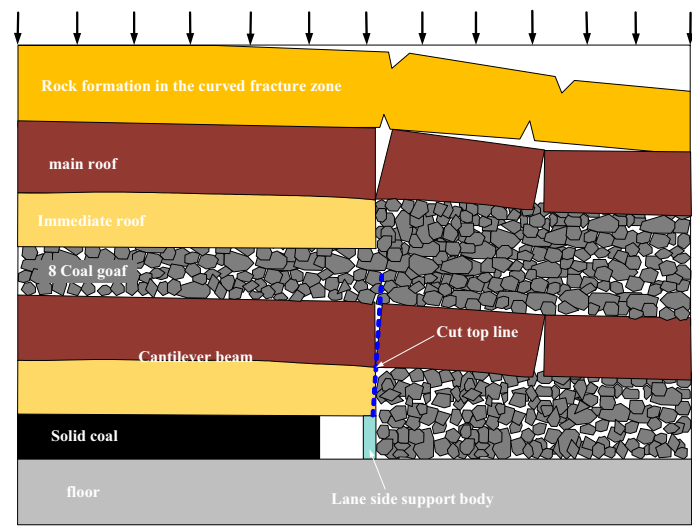
Fig. 9. Mechanical model of roof cutting along the empty roadway.

Specimen number		Diameter/mm	Thickness/mm	Pillar length/mm	Length Diameter ratio (L/D)	Radius Thickness ratio (D/t)	Eccentricity (e/mm)	Yield strength/ MPa
Concrete filled steel tube	SCL-1	83	5	1200	14.46	16.6	0	235
	SCL-2	95	5	1200	12.63	19	0	235
	SCL-3	108	5	1200	11.11	21.6	0	235
	SCL-4	121	5	1200	9.92	24.2	0	235

Table 3. Parameters of CFST long pillars.

In the case of precutting and unloading pressure on the track roadway of the 91006 working face, the calculated support resistance required for the roadway cannot be less than 3432 kN.

Study on the mechanical characteristics of high-strength support structures for roadway side

CFST pillar is used to support the gob-side roadway; when the ratio of the length to diameter (L/D) of the concrete-filled steel tube pillar is less than or equal to 4, it is generally regarded as a short pillar. Because the reserved roadway is limited by the mining height of the coal seam, the general pillar height in the medium-thickness coal seam is usually approximately 3 m. However, for large mining heights or top coal mining faces, the section height of the roadway may be as high as 4 m or even 6 m. Therefore, CFST pillar used for the gob-side roadway is a long pillar.

Experimental study on the mechanical properties of long CFST pillars

To better understand the mechanical properties of a long CFST pillar, an analysis was carried out to guide the selection of CFST pillar along the gob-side roadway. CFST-supported structures with different length–diameter ratios were selected for laboratory tests to analyse the deformation, failure and bearing characteristics of the CFST pillars. The parameters of CFST long pillars are shown in Table 3. The internal core concrete of the test piece was prepared with Portland cement to get C40 class concrete.

The exterior of the steel pipe was coated with grey antirust paint, and steel plates of 10 mm thickness were welded at both ends of the steel pipe as pillar caps and shoe plates in contact with the bearing plate of the test machine. Longitudinal and circumferential strain gauges were arranged in the middle of the steel pipe of the test piece. The test system is shown in Fig. 10. A static loading test was carried out on a long pillar pressure test machine, and a step-by-step pressurization method was adopted. The final deformation characteristics and load–displacement curves of the samples with different aspect ratios are shown in Fig. 11.

According to Fig. 11 and the analysis of the experimental phenomena, the following conclusions can be drawn:

1. Analysing the SCL-2 sample as an example, the load–displacement curve of the pillar loading process is divided into four stages: (1) the elastic stage (*oa*), which increases linearly; (2) the elastic stage (*ab*), where the load increases rapidly with increasing displacement after the pillar enters the compaction strengthening stage; (3) the plastic yield stage (*bc*), where the damage curve of the sample slowly decreases after the sample
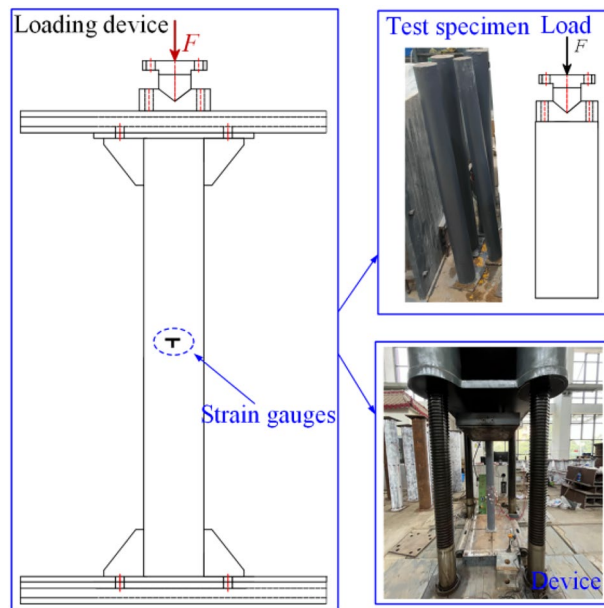
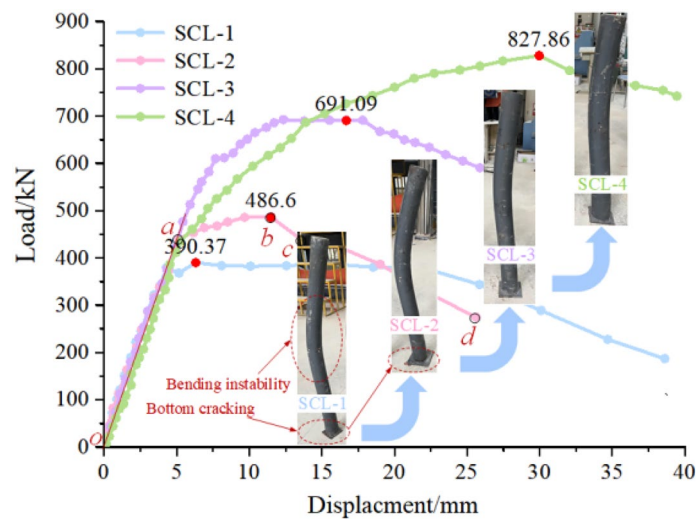**Fig. 10**. Test system.

Fig. 11. Load–displacement curves at different length-diameter ratios.

reaches the load limit; and (4) the failure stage (*cd*), where the flexural degree of the sample increases significantly and the load decreases rapidly.

2. The peak loads of the SCL-1, SCL-2, SCL-3 and SCL-4 samples are 390.37 kN, 486.60 kN, 691.09 kN and 827.86 kN, respectively, and the deformation displacements are 6.31 mm, 11.4886 mm, 16.679 mm and 29.964 mm, respectively. With decreasing length–diameter ratio, the bearing capacity of the CFST pillars gradually increases.

3. Specimens of long concrete-filled steel tube (CFST) pillars are bent and unstable to varying degrees under axial pressure. At the initial stage of loading, the load-displacement curves are essentially the same for each sample, and the length-diameter ratio has little influence on the initial deformation stiffness of the long pillar. With increasing load, specimens with larger length-diameter ratios first enter the yield stage, and cracks form at the bottom of the pillar to a certain extent. After the plastic yield stage, the load decreases rapidly, failure deformation shows the overall buckling deformation of lateral dumping, and the specimens with small length-diameter ratios clearly experience buckling deformation.

The above analysis reveals that the bearing capacity of long pillars is greatly reduced by the influence of the length-diameter ratio and that the damage to long pillars of concrete-filled steel tubes is caused mainly by the influence of bending.

Serial number		Test piece	External diameter /mm	Thickness/mm	Length/mm	Length diameter ratio	Axial compressive bearing capacity/kN
Experimental specimen	1	SCL-1	83	5	1200	14.46	397.23
	2	SCL-2	95	5	1200	12.63	512.16
	3	SCL-3	108	5	1200	11.11	650.24
	4	SCL-4	121	5	1200	9.92	802.29
Field sample selection	5	SCL-5	194	10	2600	13.40	2066.45
	6	SCL-6	219	10	2600	11.87	3907.82
	7	SCL-7	299	10	2600	8.70	4624.37
	8	SCL-8	325	10	2600	8.00	5395.92

Table 4. Calculation of bearing capacity of CFST pillars with different length-diameter ratios.
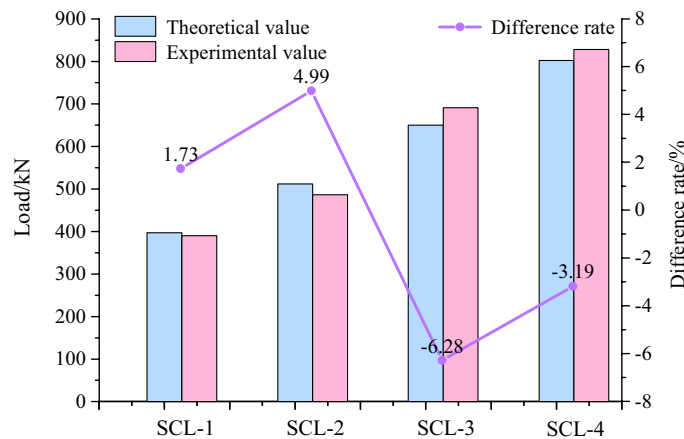

Fig. 12. The results of theoretical calculation are compared with those of laboratory test.

Calculation of the ultimate axial compressive capacity of CFST pillar

According to the theory of ultimate equilibrium, the ultimate bearing capacity of long steel-reinforced concrete columns used to support structures along gob-side roadways can be calculated via the following formula[24]:

$$N_{\mathrm{u}} = \varphi_l \cdot \varphi_e \cdot N_{\mathrm{o}} \tag{2}$$

where N_{u} is the ultimate bearing capacity of CFST long column; φ_l is the reduction factor of the influence of the slenderness ratio on the ultimate bearing capacity of the long CFST columns; φ_e is the reduction factor of the effect of eccentricity on the ultimate bearing capacity of the long CFST pillars; and φ_e is 1. N_0 is the ultimate bearing capacity of the short concrete-filled steel tube columns.

The reduction factor considering the influence of the aspect ratio on the ultimate bearing capacity of long CFST pillars can be expressed by the following empirical formula:

$$\varphi_l = 1 - 0.115\sqrt{L/D - 4} \tag{3}$$

According to the above formula, the axial compression capacity of long pillars of CFST with different length−diameter ratios is calculated, and the results are shown in Table. 4.

According to the analysis comparing the theoretical calculation results and the indoor test results in Fig. 12, the percent difference (percentage of the difference between the theoretical calculation results and the indoor test results) between the theoretical bearing capacity and experimental indoor bearing capacity of the pillar at different aspect ratios are 1.73%, 4.99%, − 6.28%, and − 3.19%, with a percent difference within ± 7%. These findings verify the correctness of the indoor test results and theoretical analysis and provide a reference for engineering applications.

On the basis of the above analysis, the final parameters for the roadside support of the short-distance goaf are determined as shown in Table 5.

Study of the deformation of the rock surrounding a close range seam roadway

To verify the feasibility of controlling the surrounding rock of goaf-retaining roadways in close range coal seam mining, FLAC 3D simulation software was used to compare the stress transfer effects of roadway roof cutting before and after fracturing and support in goaf-retaining roadways and to clarify the control mechanism of gob-side roadways in close range coal seam mining.

Region	Design scheme	Design parameters
Roadway-side supporting	Concrete-filled steel tube pillar	Q235 seamless steel pipe, size $\Phi 299 \times 10$ mm, theoretical bearing capacity of the pillar 4624kN (can not be lower than the theoretical value of the abutment pressure of the supporting body beside the roadway 3432 kN), filling core concrete C40, spacing 800 mm

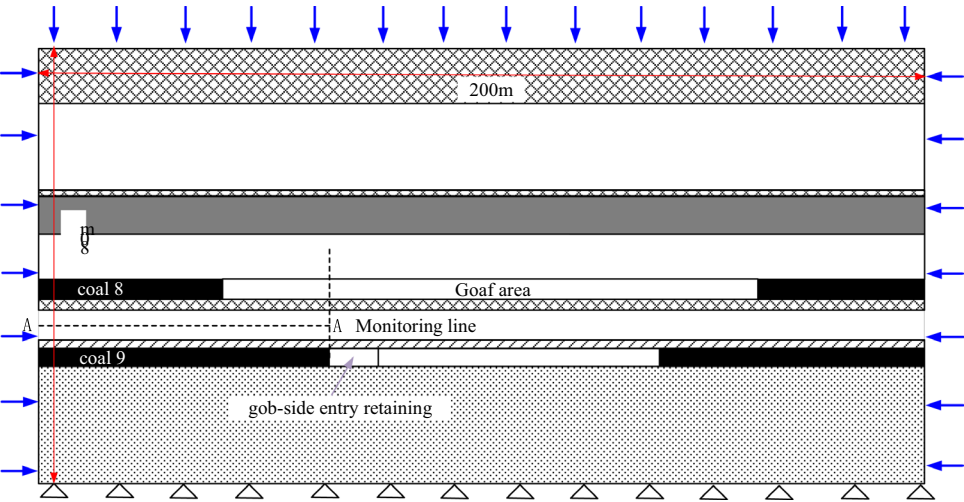**Table 5**. Support design scheme and parameters.

Fig. 13. Numerical model diagram.

Numerical simulation analysis of roadway retention in short-range coal seams

A numerical model was established on the basis of the engineering geological conditions of the 91006 working face. The burial depth of the No. 9 coal seam is approximately H = 350 m, with a dip angle of 0°. The 91006 working face is located 7.5 m from the upper goaf. The numerical simulation dimensions are as follows: the strike direction X of the working face, the dip direction Y of the working face, and a burial depth $Z = 160 \times 200 \times 80$ m. The width and height of the roadway are 4.1 m × 2.9 m. To reduce boundary effects, 60 m remains on each side, which is divided into approximately 48,000 units and 97,000 nodes. A roadway surrounding rock monitoring line AA' is arranged to monitor the stress changes in the rock surrounding the roadway during progress on the working face. The numerical model is shown in Fig. 13. The upper surface of the rock model is the stress boundary, and a uniform load is applied to the model to simulate the self-weight of the overlying rock mass strength. The bottom of the model is fixed, and the normal direction is fixed for other boundaries. The Mohr–Coulomb is effective in characterizing the elastic–plastic behavior of geotechnical materials, and its parameters are easy to obtain through experiments. It has strong engineering applicability and can accurately evaluate the stability of surrounding rock and support requirements. The Mohr–Coulomb model was selected as the surrounding rock model, and the mechanical parameters are shown in Table 1. Although solid elements can simulate any object, it is very difficult to achieve bending moments. Therefore, the pillar adopts a beam structural element, with a top cutting hole length of 11 m, a cutting angle of 35°, a drilling hole diameter of Φ65, and a drilling spacing of 6000 mm.

The numerical simulation for roof cutting and pressure relief along the goaf in the lower area of the close range goaf includes the following five steps: ① analysis of original rock stress balance; ② calculation after the backfilling of the 8th coal seam working face; ③ after excavating to the 91006 working face roadway, the 91006 working face will be mined again; ④ at the top of the roadway near the goaf in 91006 track roadway, construction is carried out with an elevation angle of 65° perpendicular to the direction of the working face, advancing 6 m each time, and performing roof cutting treatment. 100 Steps are calculated each time, until all roof cuttings are completed, and then the model is calculated to balance; ⑤ insert structural unit next to the 91006 track roadside for support and calculate until the model is balanced. Analyze the stress distribution and plastic zone distribution of the surrounding rock along the goaf under different support conditions before and after top cutting. The different simulation schemes and parameters are shown in Table 6.

Vertical stress distribution law
According to the analysis in Figs. 14 and 15, the stress peaks in Plans A, B, C and D are 34.2 MPa, 23.5 MPa, 26.7 MPa and 19.9 MPa, respectively. Roadway side supporting and roof cutting techniques reduce the

Scheme	Roof cutting	Steel composite pillar support	Top cutting parameter/mm				Parameters of concrete-filled steel tube pillar/mm		
			Diameter	Length	Angle	Spacing	Diameter	Thickness	Height
Plan A	None	None	–	–	–	–	–	–	–
Plan B	Yes	None	65	11,000	35	6000	–	–	–
Plan C	None	Yes	–	–	–	–	299	10	2600
Plan D	Yes	Yes	65	11,000	35	6000	299	10	2600

Table 6. Design scheme and parameters.
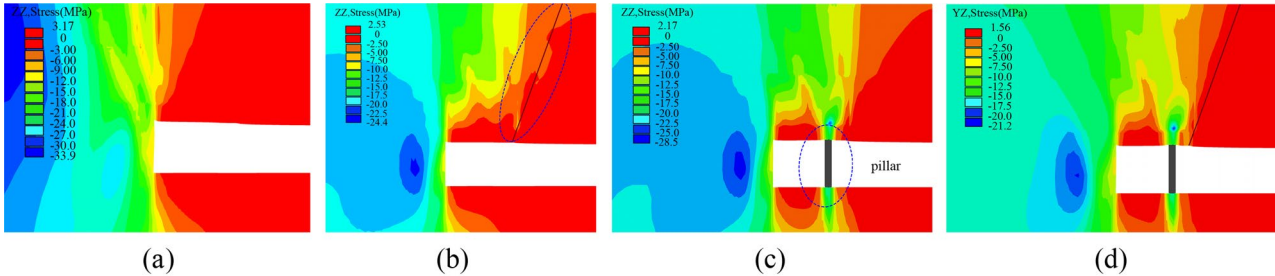
Fig. 14. Vertical stress evolution cloud map of different schemes.
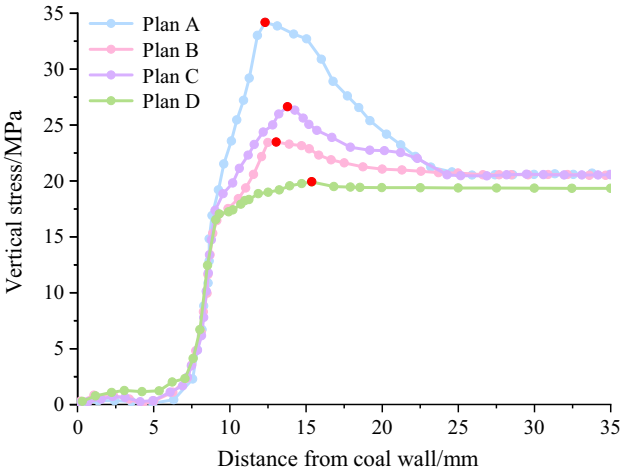
Fig. 15. Supporting pressure curve chart.

concentration of lateral stress to a certain extent, and the pressure relief area is farther from the lane-retaining area and transferred to the depth of the gob. As a carrier, a concrete-filled steel tube pillar shares part of the mining pressure experienced due to rock movement, for example, resulting in the minimum degree of abutment pressure concentration, and the peak abutment pressure decreases by 42.8% compared with that of no roadway and decreases by 31.2% compared with that of no roadway and no tangential ratio. The ratio is reduced by 21.9%, which indicates that hydraulic fracturing of the top relief and high-strength support of CFST pillars can effectively reduce the mining stress of the working face rock and reduce the surrounding rock pressure to optimize the surrounding rock stress environment in roadway retention.

Shear stress analysis law
According to the analysis of the shear stress maps of the different schemes in Fig. 16, Scheme A has a smaller range of shear stress bands and smaller shear stress values. The shear stress value within the stress band is approximately 5.68 MPa. The shear stresses of schemes B, C, and D are 6.81 MPa, 7.16 MPa, and 8.98 MPa, respectively, and the range of shear stress bands gradually increases. The above analysis reveals that the existence of support structures and top roof cutting pressure relief in the roadway causes the shear stress zone of the roof to shift towards the goaf side, and longitudinal cracks in the rock mass develop within the shear stress concentration zone, providing conditions for fracture failure and rotational subsidence of residual rock blocks in the lateral direction. This finding indicates that the support structure along the roadway and the top cutting
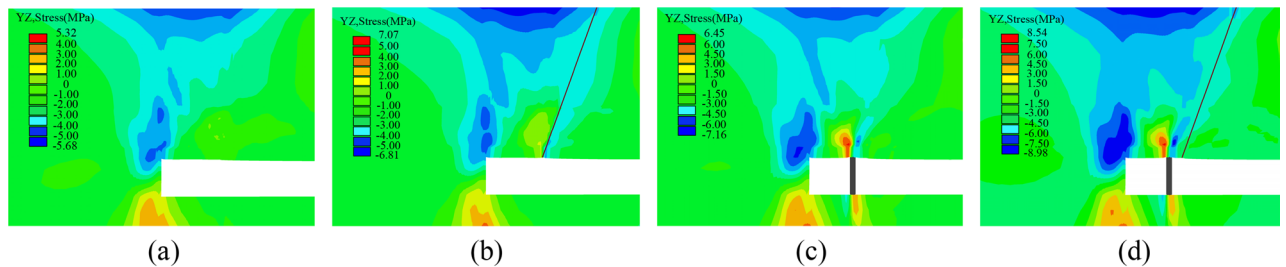
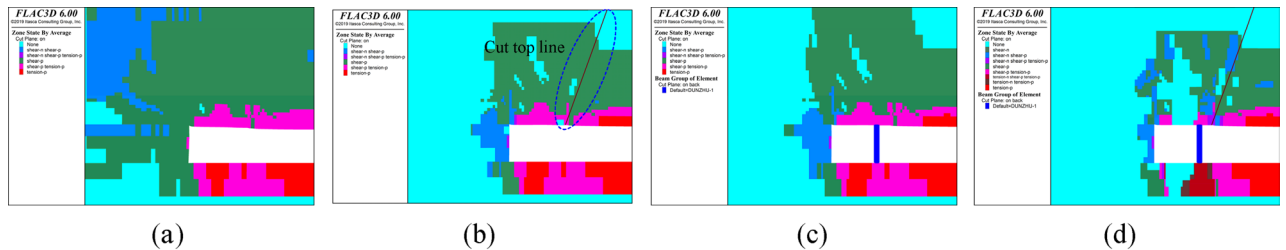**Fig. 16**. Diagram of shear stress on the roof of different schemes.

Fig. 17. The overall plastic zone of the top and bottom plates in different schemes.
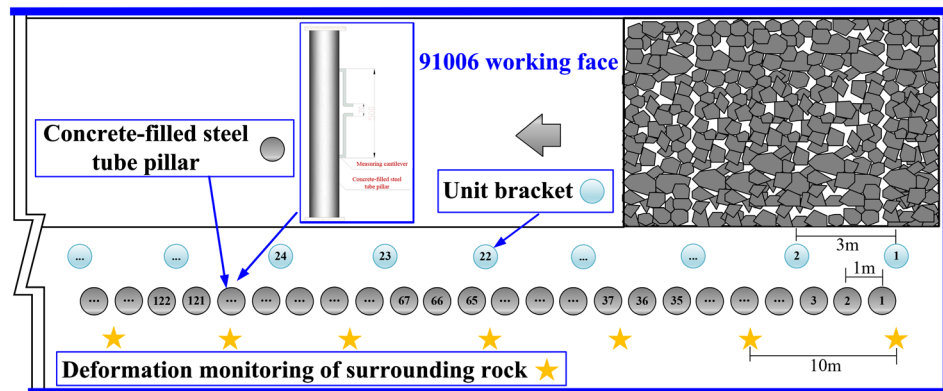

Fig. 18. Monitoring layout diagram.

pressure relief effectively control the damage to the surrounding rock of the goaf-retaining roadway and that the combination of the two has a more significant effect.

Plastic region distribution

Figure 17 shows the plastic zones generated by the top and bottom plates of different schemes for retaining tunnels along the goaf. The top and bottom plates of Scheme A fully enter the plastic state, indicating that the roof is prone to collapse. The top and bottom plate areas of Scheme D remain intact, further indicating that the combination of hydraulic fracturing and top cutting and pressure relief with high-strength support of concrete-filled steel tube pillars for retaining tunnels along the goaf has a good effect.

Analysis of field measurements of roadway retention in short range coal seams

To ensure the safety of the roadway, real-time monitoring of the deformation of the surrounding rock and composite support body was carried out in the test section of the empty roadway along the track groove of the Xinchazhuang 91006 working face. Two monitoring stations are arranged for mine pressure monitoring, which monitors the manifestation of mine pressure during the process of retaining the roadway through surface displacement of the roadway (employing cross-point measurement), deep displacement of the roadway (utilizing multi-point borehole sensors), and working resistance of the support body (monitored by pressure gauges)[25,26]. In response to the control requirements of the support body on the rock surrounding the roadway, the monitoring layout is shown in Fig. 18.
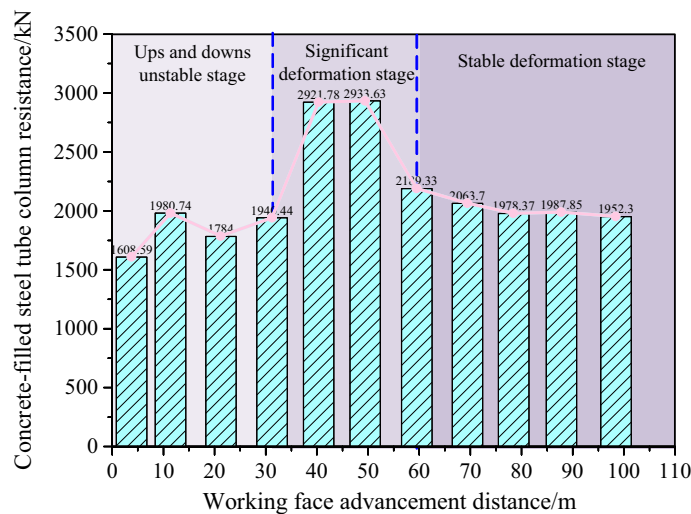
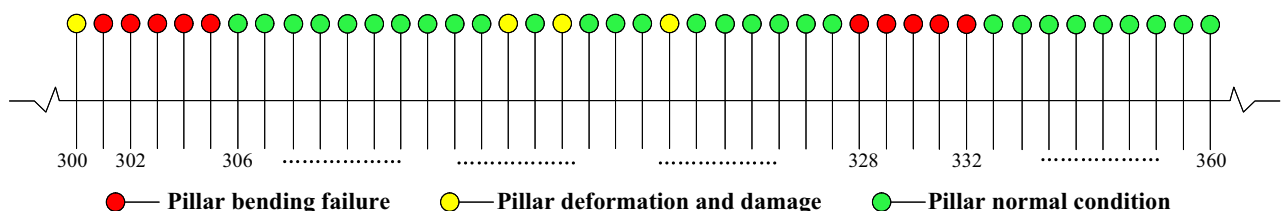**Fig. 19**. Force curve of concrete-filled steel tube pillar.

Fig. 20. Damage diagram of concrete-filled steel tube pillar.

Analysis of the resistance change of the high-strength support of a CFST pillar beside a roadway
The loading curve of CFST pillar is shown in Fig. 19. With the advancement of the working surface, the force of CFST pillar presents three stages: 0–30 m is the fluctuating and unstable stage. At this time, the concrete is still in the grouting solidification stage, the bearing capacity is low, the lag working face is in a significant deformation stage within 30–55 m, the roof of the roadway experiences rotation and sinking deformation, the roof of the goaf side is obviously sinking, and the force of the pillar increases. The peak support resistance of the pillar is 2933.6 kN, and theoretical needed minimum load bearing capacity is 500 kN, so it's lower by 11.7%. After 55 m, the deformation stage is stable, and the force of the pillar gradually flattens and becomes stable.

Figure 20 shows the extent of damage of CFST pillar. When advanced mining of the first working face has an impact on the pillar, the surrounding rock of the roadway is subjected to loading action, which causes the abutment pressure to transfer from the surface to greater depths. Because the stress concentration coefficient of advanced mining is significantly greater than that of excavation, the range of surrounding rock affected by the load greatly increases, which leads to an increase in the pressure on the pillar, and finally, bending deformation occurs. As shown in the analysis of Fig. 20, the pillar section No. 332-360 transitions from the advanced supporting pressure in the primary mining stage to the lagging support pressure stage. The range of influence of the initial pressure step is between pillars No. 328 and 332, and the range of influence of the first pressure step and the second cycle pressure step is between pillars No. 300 and 328. In the period behind the working face, when the immediate roof is damaged above the solid coal body, the roof rebounds, and the surrounding rock is also unloaded, thus forming an internal and external stress field on the side of the solid coal body. On the basis of the whole supporting pillar, the roof of the whole roadway is intact, and because the two sides are not close enough, the roadway is successfully retained. From each part of the support, the bending failure rate of the new pillar is reduced from the original 50–70% to 20–35%, which effectively reduces the bending failure of the pillar and achieves a better supporting effect.

Analysis of the overall deformation law of rock surrounding a roadway
According to the roadway surface displacement monitoring shown in Fig. 21, as the working face advances, the surface displacement monitoring curve rises rapidly, with a duration of approximately 8 days. The average deformation rate of the roof and floor is 2.33 mm/d, and the average deformation rate of the two sides is 2.8 mm/d. As it moves away from the excavation working face, the deformation speed of the surrounding rock decreases continuously. When it is approximately 110 m from the working face, the deformation of the surrounding rock tends to stabilize, and the excavation influence period is approximately 22 days. After the roadway reaches a
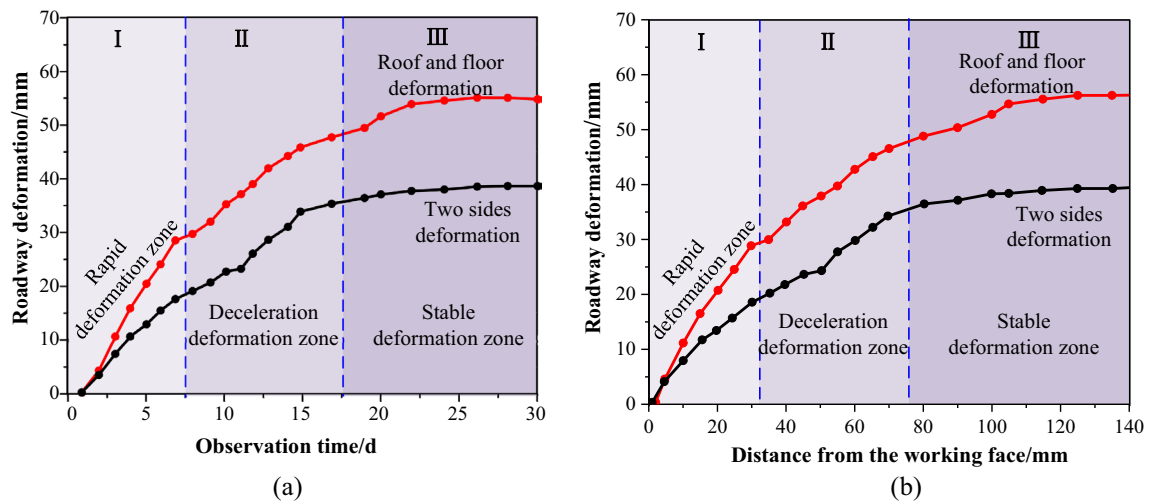
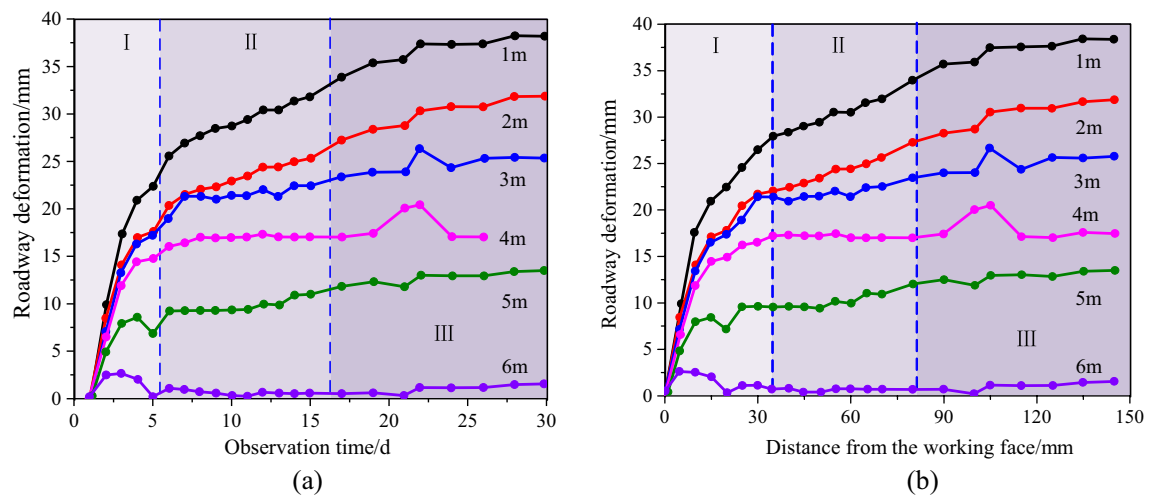**Fig. 21**. Roadway surface displacement monitoring curve.

Fig. 22. Monitoring curve of deep surrounding rock displacement.

stable state, the deformation speed of the surrounding rock is basically 0, the deformation of the roof and floor is 57 mm, and the deformation of the two sides is 38 mm.

Borehole sensors are instrumented with six measurement points at 1 m intervals (1–6 m depth). According to the displacement monitoring of the deep surrounding rock in Fig. 22, the range of movement of the roof in the tunnel direction is 6 m. The maximum deformation of the surrounding rock towards the tunnel measured beyond 6 m is relatively small, at only 0–2 mm. The deep surrounding rock is basically stable, and within 0–5 m of the rock surrounding the tunnel, the deformation gradually decreases from the surface of the tunnel towards the deep area. The displacement of the deep surrounding rock gradually becomes more stable with increasing distance from the working face. At a distance of approximately 110 m, the deformation of the deep surrounding rock has essentially stabilized, and the stabilization time is essentially the same as the stabilization time of the surface displacement of the surrounding rock. The displacement of the surrounding rock in the roadway is within a safe and controllable range and does not affect the next mining face or roadway reuse.

Analysis of field applications
The pictures demonstraining the field support effect are shown in Fig. 23. The combination of top roof cutting pressure relief and high-strength composite support along the roadway was successfully applied in the Xinchazhuang mine, with good results overall, promoting research on and the application of close range goaf retention technology and further improving the efficiency and safety of coal mining.
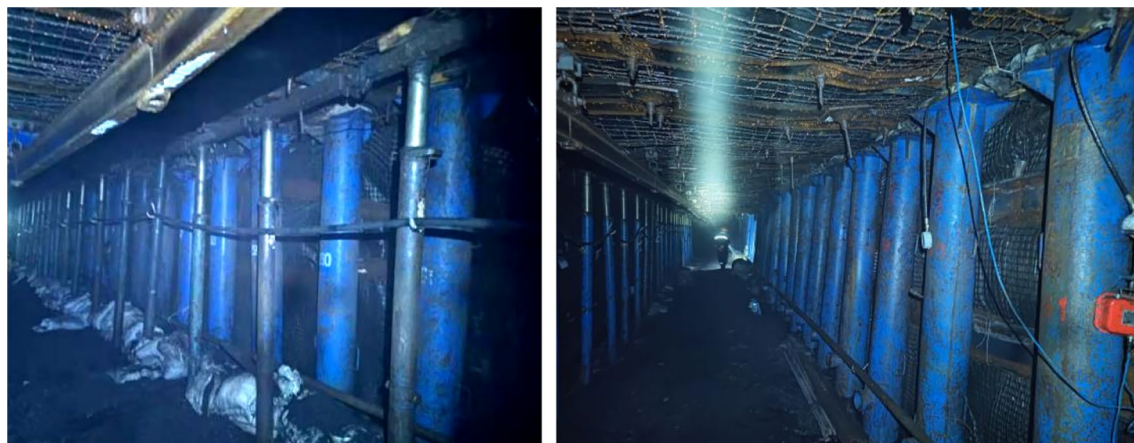
Fig. 23. Field support effect in the roadway.

Conclusion

1. On the basis of the theory of overlying rock combination structures and advanced roof unloading technology, a modified mechanical model of the overlying rock structure roadside was established, and a precise quantitative support design method for the surrounding rock without coal pillars was constructed, featuring rock mechanical performance, support strength design, and structural optimization as a main steps.

2. To further verify the reliability of high-strength concrete-filled steel tube (CFST) pillars as gob-side roadway support structures, theoretical and experimental research were carried out on the failure forms and mechanical properties of long CFST columns under axial compression with different L/D ratio, laying the foundation for a reasonable selection of CFST pillars. The long CFST column presents an overall bending failure mode. With decreasing L/D ratio, the deformation and failure characteristics of the sample remain essentially unchanged, and the failure of the pillar is affected by compressive bending. However, the ultimate bearing capacity gradually increases.

3. Proposed hydraulic fracturing combined with high-strength composite support method for roadway retention in close range coal seam that used hydraulic fracturing to cut off the top plate of the goaf, causing the overlying rock to rotate, sink, and deform. The fracture structure of the top plate is actively transformed from a transmitting rock beam to a short-arm beam structure, which greatly reduces the support pressure on the support body. In addition, the combination of high-strength steel tube concrete columns strengthens the roof support of the roadway, achieving long-term stability. Industrial tests were conducted at the Xinchazhuang Coal Mine, successfully setting up a track groove, effectively reducing the amount of roadway excavation, and achieving good economic benefits.

Data availability

The data used to support the fndings of this study are available from the corresponding authors upon request.

References

1. Kang, H. P. & Gao, F. Q. Evolution of mining-induced stress and strata control in underground coal mines. *Chin. J. Rock Mech. Eng.* **43**(01), 1–40 (2024).
2. Kang, H. P. Seventy years development and prospects of strata control technologies for coal mine roadwaysin China. *Chin. J. Rock Mech. Eng.* **40**(01), 1–30 (2021).
3. Kang, H. P. et al. Strata control technology and applications of non‑pillar coal mining. *J. China Coal Soc.* **47**(1), 16–44 (2022).
4. Xu, Y. L., Pan, K. R. & Zhang, H. Investigation of key techniques on floor roadway support under the impacts of superimposed mining: Theoretical analysis and field study. *Environ. Earth Sci.* **78**, 436 (2019).
5. Lu, G. Z. & Ni, P. Support control design of mining roadway under goaf of close-distance coal seam. *Sustainability* **15**, 5420 (2023).
6. Hua, X. Z. Development status and improved proposa ls on gob-side entry retaining support technology in China. *Coal Sci. Technol.* **34**(12), 78–81 (2006).
7. Ning, J. G., Wang, J., Tan, Y. L. & Xu, Q. Mechanical mechanism of overlying strata breaking and development of fractured zone during close-distance coal seam group mining. *Int. J. Min. Sci. Technol.* **30**, 207–215 (2020).
8. Liu, W. X. et al. Research on the failure mechanism and control technology of surrounding rock in gob-side entry driving under unstable overlying strata. *Eng. Fail. Anal.* **138**, 106361 (2022).
9. Zhang, Z. Z., Deng, M., Bai, J. B., Yan, S. I. & Yu, X. Y. Stability control of gobside entry retained under the gob with close distance coal seams. *Int. J. Min. Sci. Technol.* **31**, 321–332 (2021).
10. Yin, S. F., Zheng, X. J., Wang, E., Kang, Q. T. & Zhang, X. M. Non-uniform failure and differential pressure relief technology of roadway under irregular goafs in deep close-distance coal seams. *Sci. Rep.* **13**(1), 18527 (2023).
11. Shen, F. et al. Research on key parameters of gob-side entry retaining formed by roof cutting of working face under goaf in close distance coal seams. *Min. Sci.* **29**, 19–39 (2022).

12. Hou, G. Y., Hu, T. & Li, Z. X. Effect of cutting roof height on the stability of gob-side retaining roadway with roadside support. *J. Min. Saf. Eng.* **36**(5), 924–931 (2019).
13. Han, C. et al. Multiple and long-term disturbance of gob-side entry retaining by grouped roof collapse and an innovative adaptive technology. *Rock Mech. Rock Eng.* **52**, 2761–2773 (2019).
14. Li, P. et al. Study on reasonable width and yield scale of roadway side support with strong roof and thick seam with large dip angle. *J. Cent. South Univ. (Sci. Technol.)* 53(11) (2022).
15. Yang, H. Y., Li, Y. & Liu, Y. B. Structure evolution and stability control mechanism of hard-roof cutting for roadway retaining. *J. Min. Saf. Eng.* **38**(04), 766–773 (2021).
16. Zhao, J. & Li, G. B. Pressure-relief mining of the working face under the coal pillar in the close distance coal seams. *Geotech. Geol. Eng.* **34**, 1067–1077 (2016).
17. Ma, Z. et al. Key Technologies and application test of an innovative noncoal pillar mining approach: a case study. *Energies* **11**(10), 2583 (2018).
18. Ma, Q. et al. Roadside support schemes numerical simulation and field monitoring of gob-side entry retaining in soft floor and hard roof. *Arab J. Geosci.* **11**(121), 563 (2018).
19. Zhang, N. et al. Theory and practice of surrounding rock control for pillarless gob-side entry retaining. *J. China Coal Soc.* **39**(08), 1635–1641 (2014).
20. Wang, Q. et al. Research on control methods of automatically-formed roadway without coal pillar for extremely close-distance coal seams. *J. Min. Strata Control Eng.* **6**(1), 013532 (2024).
21. Huang, W. P. et al. Technology of gob-side entry retaining using concrete-filled Steel tubular columnas roadside supporting. *J. China Univ. Min. Technol.* **44**(4), 604–611 (2015).
22. Wang, J. et al. The analysis of roadside supporting parameters and the support technology in the concrete filled steel tubular column in goaf-side entry retaining. *J. Min. Saf. Eng.* **32**(6), 943–949 (2015).
23. Sun, X. M. et al. Key parameters of gob-side entry retaining formed By roof cut and pressure releasing in Thin coal seams. *Chin. J. Rock Mech. Eng.* **33**(7), 1449–1456 (2014).
24. Wang, J. et al. Experimental study and engineering application of jacking retractable concrete-filled steel tubular column. *J. China Coal Soc.* **47**(08), 3052–3068 (2022).
25. Małkowski, P. et al. Underground monitoring as the best way of roadways support design validation in a long time period. *Min. Miner. Deposits* **14**(3), 1–14 (2020).
26. Małkowski, P., Niedbalski, Z. & Bednarek, Ł. Automatic monitoring system designed for controlling the stability of underground excavation. *Inzynieria Mineralna* **1**(2), 15–29 (2021).

Author contributions

Yaxin Liu: Original draft Wanpeng Huang: Review Tongyang Zhao: Supervision Le Sui: Formal analysis Xinyu Chu: Validation Lingzhuo Zhu: Software.

Funding

Declarations

Competing interests

The authors declare no competing interests.

Additional information

Correspondence and requests for materials should be addressed to T.Z.

Reprints and permissions information is available at www.nature.com/reprints.

Publisher's note Springer Nature remains neutral with regard to jurisdictional claims in published maps and institutional affiliations.